Journal Pre-proof

Oxidation of small aromatic compounds in rainwater by UV/H2O2: Optimization by response surface methodology

Mónica P.S. Ferreira, Patrícia S.M. Santos, Armando C. Duarte

Oxidation of small aromatic compounds in rainwater by UV/H$_2$O$_2$: optimization by response surface methodology

Mónica P.S. Ferreira, Patrícia S.M. Santos[*] `patricia.santos@ua.pt`, Armando C. Duarte

CESAM & Department of Chemistry, University of Aveiro, Campus Universitário de Santiago, 3810-193 Aveiro, Portugal

[*]Corresponding author.

Abstract

The presence of aromatic compounds in rainwater is a matter of concern, mainly when the use of rainwater in buildings is intended. The present work aimed to assess the oxidation of a mixture of small aromatic compounds (benzoic, 3,5-dihydroxybenzoic and syringic acids) in rainwater by the UV/H$_2$O$_2$ process, and the possibility of its optimization by the response surface methodology. The extent of oxidation was assessed by ultraviolet-visible and molecular fluorescence spectroscopies. During the oxidation of the mixture new chromophoric compounds were formed at an initial stage, but they were then degraded at a later stage. The increase of the H$_2$O$_2$ concentration, resulted in a higher extent of oxidation, while the initial pH value showed no influence in the oxidation of the mixture. The optimization of the oxidation was performed using the uniform design with the factors: initial H$_2$O$_2$ concentration, initial pH, and reaction time. The response surface model found, through the best subsets regression, described the extent of oxidation as function of the following variables: initial H$_2$O$_2$ concentration and reaction time, interaction between them, and also their respective quadratic forms. The optimal conditions, the lowest H$_2$O$_2$ concentration (3.1 mM) for a selected maximum reaction time (4h), were applied to rainwater samples spiked with the mixture

of contaminants and resulted in an extent of oxidation higher than 99.5%, validating the application of the model to real samples. Therefore, the UV/H_2O_2 process coupled to its optimization via response surface methodology may be an alternative for rainwater treatment in buildings.

Keywords: Rainwater; aromatic compounds; oxidation; UV/H_2O_2 process; response surface methodology.

1. Introduction

The scarcity of fresh water all over the world, due to the urban development, high water consumption, and climate change, makes imperative to find alternative water resources. Such alternatives will not reduce water use, but will allow to decrease abstraction from conventional sources (European Environment Agency, 2009).

Rainwater harvesting is a key option to alleviate the pressure on existing water resources and can help to improve the water resources sustainable management. Such type of water covers the supply of non-potable water for domestic uses, such as flushing the toilet, watering the garden, and washing clothes using a washing machine, but does not cover the supply for drinking, food preparation or personal hygiene (Environment Agency, 2010). However, for example in washing machines, if the quality of the collected water is poor, there can be issues with both colour and odour (Environment Agency, 2010). Therefore, to encourage the use of rainwater harvesting for domestic purposes it will be important to guarantee the quality of rainwater and simultaneously to expand its use, at least for personal hygiene, which will require specific guidelines. Nowadays, the European Union (EU) does not have legislation or guidelines for the use
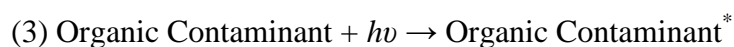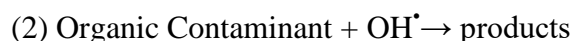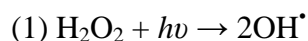
of rainwater for domestic purposes, but the use of the legislation for drinking water (Council Directive 98/83/EC) can be used as a reference.

The quality of rainwater reflects the composition of the atmosphere on a given location, in a certain time (Santos et al., 2019), and it can be affected by air masses from long range transport (Santos et al. 2011; Santos et al. 2013). However, in rainwater harvesting the quality of rainwater is also affected by the type of surface where it is collected, such as the type of roof material (Mao et al. 2021). Polyokova et al. (2018), in a recent study, showed that hundreds of organic compounds were found in Moscow's rainwater, many of them priority pollutants and emerging contaminants, such as polycyclic aromatic hydrocarbons (PAH), polychlorinated biphenyls (PCB), phenols, phthalates, phosphates, and pyridines, and that the levels of phenol, dibutylphthalate, and benz[a]pyrene have exceeded the safe values. Nevertheless, despite the concentration of contaminants in some cases being below the considered safe values, the whole of compounds present in rainwater can be harmful for the human health when this type of water is intended for domestic purposes. In fact, currently, the organic contaminants are a challenge for rainwater treatment. Therefore, efforts should be made to study the removal of organic contaminants from rainwater and to seek an efficient treatment of rainwater so that it can be used for domestic purposes with safety.

Several studies evaluated oxidation processes on the degradation of organic compounds in atmospheric waters, while natural phenomenon's occurring in the atmosphere, highlighting that they can be one way on the treatment of rainwater, namely: the combination of UV light or sunlight (SL) with Fe(III) and H_2O_2 (UV/Fe(III)/H_2O_2 or SL/Fe(III)/H_2O_2), for the oxidation of oxalic acid by Zuo and Holgné (1992); the UV alone, or the combination of UV or SL and Fe(III), for the oxidation of benzoic acid by Deng et al. (2006); the combination of UV/Vis light with and without NO_3^-, for the

degradation of 4-nitrophenol by Vione et al. (2009); the combination of UV light and H_2O_2, for the oxidation of pyruvic acid by Boris et al. (2015); the combination of Fe(III) with H_2O_2, for the oxidation of benzoic acid, 4-hydroxybenzoic acid and 3,5-dihydroxybenzoic acid by Santos and Duarte (2015); the combination of Fe(III) with H_2O_2, for the oxidation of vanillic acid and syringic acid by Santos et al. (2016) and Zhao et al. (2022); the oxidation of benzoic acid with H_2O_2, Fe (III) and SL, and combination of the previous ones by Santos et al. (2019). To the best of our knowledge, the study of Santos et al. (2019) was the only one that studied the oxidation of organic contaminants in rainwater (while natural phenomenon), and showed that the combination of the oxidants (SL/Fe(III)/H_2O_2) accelerated the degradation of benzoic acid, with the sunlight being essential on the high extent of oxidation, which highlights that the light is important for the degradation of organic contaminants in these type of waters.

The UV/H_2O_2 advanced oxidation process (AOP) has been widely evaluated for the oxidation of organic contaminants in water (e.g. Wang et al., 2019; Ding et al., 2020; Mangalgiri et al., 2021). In this process, the hydroxyl radical, photogenerated by the UV/H_2O_2 process, is pointed out as the main responsible for the oxidation of organic compounds (reactions 1 and 2). The reactive chemical specie generated, $OH^\bullet$, can degrade the organic molecules and mineralize them to CO_2 and H_2O. Nevertheless, UV direct photolysis can also contribute to the degradation of an organic contaminant in a UV/ H_2O_2 AOP (reactions 3 and 4).

(1) $H_2O_2 + h\upsilon \rightarrow 2OH^\bullet$

(2) Organic Contaminant + $OH^\bullet \rightarrow$ products

(3) Organic Contaminant + $h\upsilon \rightarrow$ Organic Contaminant*

(4) Organic Contaminant* $\rightarrow$ products

To the best of our knowledge, only Li et al. (2016) studied the efficiency of the H_2O_2/UV process in rainwater treatment for its posterior use. The purpose of the study was to remove two aromatic compounds, phenol and para-Chlorobenzoic Acid (pCBA) in rainwater, and showed high efficiency on phenol and pCBA removal, with a removal efficiency higher for phenol than for pCBA. Furthermore, this study indicated that higher UV intensity or a longer irradiation period would be necessary for the effective total organic carbon removal. Liu et al. (2020) also evaluated the use of the H_2O_2/UV process but for controlling disinfection by-product (DBP) formation in rainwater during post-chlorination and showed that such process change the DOM characteristics in rainwater leading to the efficient control of DBP formation. In addition, either UV light or H_2O_2 are both conventional disinfection processes, and Fiorentino et al. (2021) showed that both UV-C radiation and H_2O_2 combined with sunlight (sunligth/H_2O_2) processes inactivated *E. coli* and Entero strains in rainwater, with the sunlight increasing the inactivation, which also highlights the potential of these oxidants on disinfection of rainwater. Because the H_2O_2/UV process has the advantages of not introducing secondary pollutants, and that it can be simultaneously used for the degradation of organic contaminants (Li et al., 2016) and for the disinfection of water matrices (Kokkinos et al. 2021), such process should be more investigated in what concerns to its usage for the treatment of rainwater. Therefore, it is of utmost importance to evaluate the parameters that affect the H_2O_2/UV process, namely pH of water, concentration of H_2O_2, and time of oxidation, as well as to evaluate the possibility of its optimization for rainwater treatment.

Response surface methodology (RSM) by uniform experimental design has been successfully applied on the optimization of processes in many industrial and scientific experiments (Li et al., 2004). This experimental design allows the design points to

scatter uniformly on the experimental domain, which has the advantage that, in a small number of runs, a large amount of information can be acquired (Li et al., 2004). For the analysis of the resulting data, the best subsets regression approach can be used. This is a model selection approach that tests all possible combinations of predictor variables, and, based on some statistical criteria (e.g. adjusted R^2, R^2 and C_p) selects the best models for each number of possible predictors.

To the best of our knowledge, the possibility of the optimization of the organic contaminants oxidation with the UV/H_2O_2 process, by response surface methodology, has not been evaluated for rainwater, but it could be of the greatest importance when the applicability of the process to a real context is desired. The aims of this work were to evaluate the oxidation of a mixture of organic contaminants in rainwater by the UV/H_2O_2 process and to assess the possibility of the optimization of the process using a response surface methodology to be used for rainwater treatment. The mixture was composed by small aromatic compounds, benzoic acid, 3,5-dihydroxybenzoic acid and syringic acid, which are tracers of biomass burning (Simoneit, 2002) and that have been found in aqueous extracts of biomass burning aerosols (Graham et al., 2002). The oxidation of contaminants was performed in water model solutions and in real rainwater samples, and was evaluated by Ultraviolet-Visible (UV-Vis) and molecular fluorescence spectroscopies. The effects of pH of water, initial concentration of H_2O_2, and time of reaction on the oxidation of contaminants were assessed. For the optimization of the process of degradation of the mixture of contaminants in rainwater by UV/H_2O_2 process, the Uniform Design was employed, followed by the best subsets regression approach.

2. Material and methods

2.1. Experimental procedure

The oxidation of a mixture of compounds containing benzoic acid, 3,5-dihydrozybenzoic acid and syringic acid, each one with a concentration of 0.02 mM, was performed in water model solutions and in rainwater samples, under UV radiation (254 nm) and in the presence of H_2O_2 (UV/H_2O_2 process). Solutions were freshly prepared from stock solutions of benzoic acid (10 mM), of 3,5-dihydrozybenzoic acid (10 mM), of syringic acid (2 mM) and of H_2O_2 30 % (w/w). After the preparation of the solutions, the pH was always measured and adjusted with H_2SO_4 (0.1 M) and $NaHCO_3$ (0.1 M) solutions. A pH meter with a glass Jenway pH electrode (model 924 005) was used and calibrated each day of experimental work with pH 4 and pH 7 buffers. After adjustment of pH, 20 mL of the solutions were transferred to quartz test tubes, H_2O_2 was added and, immediately after, the tubes were put in an incubator at (20 ± 2) ºC to initiate the oxidation reactions under a 6 W UV lamp emitting at 254 nm.

To assess the effect of the reaction time, after adjustment of pH to 5.6 (neutral pH for rainwater), H_2O_2 was added to obtain an initial concentration of 0.5 mM (in the range of H_2O_2 concentration found in the atmospheric aqueous phase, 10^{-6}–10^{-4} M; Vione et al., 2006), and the oxidation was evaluated for the following reaction times: 0 h, 0.5 h, 1 h, 1.5 h, 2 h, 3 h, 4 h, 5 h, 6 h and 7 h. The final reaction time of 7 h was chosen because it was the time needed to completely degrade all the chromophoric compounds with the H_2O_2 concentration of 0.5 mM. At least three replicates of the above procedure were made in different days. In a similar way, the oxidation was also performed for the individual compounds as control (see Supplementary Material (SM), Fig. SM-1, Fig. SM-2). Three different concentrations of H_2O_2 were tested, namely: 0.5 mM, 2.5 mM and 5.0 mM. These concentrations were selected since, the lowest concentration is a typical value in atmospheric water (Vione et al., 2006), the highest concentration was

found to be able to remove a contaminant from rainwater in another study of ours (data not shown), and the concentration at middle (2.5 mM) was chosen to be half of the highest concentration. The steps were the same as referred above, and the oxidation was evaluated for 0 h, 1 h, 2 h and 4 h, since, when using the two higher H_2O_2 concentrations, 4 h is the time required to degrade almost all chromophoric compounds. To test the effect of pH, three different initial pH's were used, namely, 4.0, 5.6 and 7.0, which are acid, neutral, and basic pH values for atmospheric waters, respectively (Seinfeld and Pandis, 2006). The initial concentration of H_2O_2 was fixed at 5.0 mM, and the oxidation was evaluated for 0 h, 1 h, 2 h, 3 h and 4 h. At least three replicates were made for each pH. The effects of the reaction time, of the initial H_2O_2 concentration and of the initial pH, on the oxidation of the mixture of compounds, were assessed by UV-Vis and molecular fluorescence spectroscopies.

Prior to use, all glass material was immersed in a solution of NaOH (0.1 M) for 30 min, and then, rinsed with distilled water, followed by another immersion in a solution of HNO_3 (4 M) for 24 h, after which the materials were rinsed with distilled water and with ultrapure water.

2.2. Optimization of the oxidation of contaminants using Uniform Design

The uniform experimental design was used for the optimization of the removal of contaminants by UV/H_2O_2, and three levels for three factors were defined. The factors were the reaction time, the initial H_2O_2 concentration and the initial pH of solution, and the levels used were the following: 2 h, 4 h and 7 h, for the reaction time; 0.5 mM, 2.5 mM and 5.0 mM, for the H_2O_2 concentration; and 4.0, 5.6 and 7.0, for the pH of solutions. The response variable was the extent of oxidation, calculated based on the integrated excitation-emission matrix (EEM) fluorescence spectra volume, as follows:

$$Extent\ of\ oxidation\ (\%) = \left(1 - \frac{V_t}{V_0}\right) \times 100 \#(1)$$

where V_t is the integrated EEM fluorescence spectra volume during the reaction, at a

time t, and V_0 is the integrated EEM fluorescence spectra volume at the initial time of

reaction (0 h). A $U_{12}(3^3)$ design was applied (Table 1), and three replicates of the design

were performed in different days.

The experimental data were analysed using the best subsets regression approach, in

order to find the "best subsets". For such, three predictors were incorporated for the

model selection, as well as their interactions between each other and quadratic forms,

which represents a total of nine predictors to incorporate in the model. This translates

into the search for the "best model" with up to nine predictor variables. Thus, the result

was a list with the best model with one variable, the best model with two variables, and

so on, up to a model with nine variables. After their determination, regression analyses

were executed for each regression model, to determine the significance level of each

predictor variable. MINITAB (version 18) trial version was used for the best subsets

regression and for the regression analyses. A model was obtained with a second order

polynomial equation, which considers the interaction between the variables, and that

can be expressed according to Equation 2:

$$Y = \beta_0 + \sum_{i=1}^{k} \beta_i x_1 + \sum_{i=1}^{k} \beta_{ii} x_{ii}^2 + \sum_{i \leq j}^{k} \sum_{j}^{k} \beta_{ij} x_i x_j + \varepsilon \#(2)$$

where i is the linear coefficient, j is the quadratic coefficient, β is the regression

coefficient, k is the number of factors studied and optimized in the experiment and ε is

the random error (Kasiri et al., 2008). Working-Hotelling confidence intervals, with a

significance level of 95 %, were applied to the model, according to the equation

(Deming and Morgan, 1987):

$$\hat{y}_{10} = X_0\hat{B} \pm \sqrt{W^2 \times s_r^2[X_0(X^TX)^{-1}X_0^T]} \#(3)$$

where $\hat{y}_{10}$ is the true mean value of response; X_0 is a matrix that comprehends only one row, with columns corresponding to the columns of the X matrix, which is the matrix of parameter coefficients for each experiment; $\hat{B}$ is the matrix of parameter estimates; s_r^2 is the variance of residuals; and W^2 is the result of the multiplication of the number of parameters (p) by the tabular value of $F_{(p,n-p)}$.

The identification of the optimum conditions was achieved using Python 3.7, by resolving the model equation for expected percentages of extents of oxidation equal or higher than 99.5 %. The outcome of this procedure was a list of several optimum conditions, from within an equilibrium between the initial H_2O_2 concentration and the reaction time was searched, in order to have a minimum H_2O_2 concentration for a maximum reaction time of 4 h.

2.3. Test of the UV/H_2O_2 process in rainwater samples

Two rainwater samples were collected at a sampling station located on the University of Aveiro's campus, in the western part of the town of Aveiro, Portugal (40º38'N, 8º39'W), on 5 and 6 April 2019 (samples 1 and 2, respectively). Rainwater sampling was carried out 70 cm above the ground, through glass funnels (30 cm diameter) into glass bottles (5 L), placed inside PVC (polyvinyl chloride) opaque tubes, to ensure protection from direct sunlight and to minimize changes due to photochemical reactions (Santos et al., 2013). Four collectors of rainwater were left out open at 10 h of local hour, during a period of 24 h, and both wet and dry depositions were collected. After collection, the samples were divided into two aliquots. One of the aliquots was used for the immediate measurement of the pH and electrical conductivity (σ). A second aliquot was filtered through hydrophilic PVDF (polyvinylidene fluoride) Millipore

membrane filters with 0.45 μm of pore size, and a fraction of this volume was used for the immediate optical analysis (UV-Vis and molecular fluorescence spectroscopies). The remaining volume was frozen for posterior analysis.

Experiments with the two rainwater samples at their natural pH were performed in a similar way to what was described for model solutions, to test the influence of the matrix on the oxidation of the mixture of contaminants by the UV/H_2O_2 process. For such, samples were spiked with the contaminants (benzoic acid, 3,5-dihydrozybenzoic acid, and syringic acid, each one with a concentration of 0.02 mM) and H_2O_2 was added (to obtain a concentration of 5.0 mM) to initiate the reaction. The oxidation was evaluated for the reaction times of 0 h, 2 h and 4 h. Control experiments were also performed in a similar way for: samples, samples spiked with H_2O_2 and samples spiked with the mixture of contaminants but without H_2O_2. Additionally, experiments at the optimum conditions (3.1 mM of H_2O_2 and 4 h of reaction time) were carried out for both samples spiked with the mixture of contaminants, and two replicates were made.

2.4. Optical analysis

UV-Vis spectra, in the range of 200-500 nm, were recorded on a Shimadzu (Dusseldorf, Germany) Model UV-210PC spectrophotometer using quartz cells of 1 cm path lengths for the oxidation experiments, and of 10 cm path lengths for the rainwater samples. Ultrapure water was used as reference, to obtain the baseline.

The molecular fluorescence spectra were obtained using a Jasco FP-6500 spectrophotometer with a xenon lamp as the source of radiation and using 1 cm quartz cells. Excitation-emission matrix (EEM) fluorescence spectra were obtained by concatenating emission spectra measured every 5 nm from 230 nm to 500 nm using excitation wavelengths from 220 nm to 450 nm, increasing at 10 nm intervals. The

spectra were recorded at a scan speed of 500 nm min^{-1}, using 5 nm band widths on both

the excitation and emission monochromators. For each day of experimental work, the

fluorescence blank spectrum (ultrapure water) was subtracted from the solutions

spectra.

3. Results and discussion

3.1. Effect of time of reaction on the oxidation

Fig. 1 (a) and 1 (b) show the UV-Vis spectra and the synchronous fluorescence spectra,

respectively, of the mixture of contaminants, containing benzoic acid, 3,5-

dihydroxybenzoic acid and syringic acid (BA, DHBA and SA, respectively), during the

oxidation by UV/H$_2$O$_2$, at an initial pH value of 5.5 and with an initial H$_2$O$_2$

concentration of 0.5 mM. As shown in Fig. 1 (a), the spectrum recorded at 0 h of

reaction presents a single absorption band, located at about 251 nm, which results from

the overlapping of the individual bands of each compound (see SM, Fig. SM-1). In fact,

such band is due to the π-π* electronic transitions of the compounds in the mixture,

associated with their benzene rings and with their substitutions by the carboxylic group,

hydroxyl group and methoxy group (Williams and Fleming, 1989; Santos and Duarte,

2015; Santos et al., 2016). After 0.5 h of reaction, this band disappears, and a new band

appears at longer wavelength of 290 nm, which, after 3 h of reaction, also disappears.

The overall absorbance of the spectra continues to decrease until the end of the reaction

(7 h). These findings suggest the occurrence of chemical reactions during the oxidation,

and that the degradation of the compounds is occurring with the course of the reaction

time.

Fig. 1 (b) shows that, at the initial time, the synchronous fluorescence spectrum presents

two fluorescence bands, one is located at 270 nm (which is the location of the

fluorescent band of syringic acid, see SM, Fig. SM-2), and the other is submerged in this one, at about 290 nm (which is the location of the fluorescent band of DHBA, see SM, Fig. SM-2). After 0.5 h of reaction, the intensity of the bands significantly decreased, and the formation of new compounds is suggested by the appearance of two new bands. These new bands are located at longer excitation wavelengths, namely at 340 nm and 405 nm, suggesting that the compounds formed are more complex than the previous ones, possibly with higher substitution of benzene ring by hydroxyl groups, which was also suggested during the Fenton-like oxidation in the absence of light of BA, DBHA and SA in model atmospheric waters (Santos and Duarte, 2015; Santos et al., 2016) and during the oxidation of BA with sunlight in rainwater samples (Santos et al., 2019). With the course of reaction, the initial bands continue to decrease their intensities until they disappear, and within 7 h, only vestigial signals of the bands at 340 nm and 405 nm of excitation are present, suggesting that a very low content of chromophoric compounds remains in solution. The course of the reaction is better understood by the EEM fluorescence spectra of the mixture throughout the UV/H_2O_2 oxidation process, as shown in Fig. 2. In fact, the fluorescence spectrum at the initial time evidences the overlapping of the bands of the individual compound (see SM, Fig. SM-2). Moreover, Fig. 2 highlights that after 0.5 h of oxidation the initial chromophoric compounds are in the process of transformation, which is visible by a fluorescent trace linking the initial bands to two new bands. This fluorescent trace starts to disappear in the spectrum of 1 h, and the new bands can now be clearly seen one is found at 240 nm of excitation and 420 nm of emission, and the other one at 300 nm of excitation and 415 nm of emission wavelength. These new bands were also observed in the spectrum of the oxidation of BA at a similar reaction time, since the fluorescent bands formed during the BA oxidation spectra have a higher intensity than the bands present in the spectra of

DHBA and SA (see SM, Fig. SM-2), which possibly overlap the bands resulting from the oxidation of these lasts compounds. In the spectra of the mixture, the main fluorescent band (300 nm of excitation and 415 nm of emission wavelength), moves to longer excitation wavelengths during the reaction and another fluorescent band seems to be submerged in this one. After 3 h of reaction, the intensity of the bands starts to decrease, and the band previously found at 300 nm of excitation and 415 nm of emission moves to 320 nm of excitation and 445 nm of emission, which are wavelengths similar to the bands obtained from the oxidation of the three compounds when alone (see SM, Fig. SM-2). These results suggest that similar compounds are formed during the oxidation of the mixture and of the compounds when oxidized separately. As mentioned above, the dislocation of the fluorescence bands to longer excitation wavelengths, suggests that the compounds formed have higher complexity than the original compounds, and higher substitution of benzene rings by electron-donator groups, such as hydroxyl (Santos and Duarte, 2015). With the course of reaction, the intensity of the bands present in the spectra of the mixture continues to decrease, and after 7 h of reaction, almost all chromophoric compounds seem to be degraded. These findings show that, during the oxidation by UV/H_2O_2, the mixture of compounds is oxidized throughout time. However, while within 4 h the three compounds when oxidized alone seem to be completely degraded (see SM, Fig. SM-2), at least in what regards to chromophoric compounds, the mixture of the three acids requires 7 h of reaction to achieve similar outcomes. This could be explained by the fact that, in the mixture, there is a higher content of compounds in solution for the same amount of hydroxyl radicals. On this scenario, H_2O_2 could be acting as the limiting reagent, but the occurrence of parallel reactions, or competition for the chemical oxidants and/or UV, could also cause the reaction to be slower (Boris et al., 2015;

Santos et al., 2019). In fact, besides the oxidation of the mixture of compounds by the action of hydroxyl radical from H_2O_2, the oxidation also occurs in the presence of UV light alone as oxidant (see SM, Fig. SM-3), but the oxidation is much slower, corroborating the occurrence of parallel reactions by the action of the UV light. Moreover, these findings highlight the importance of UV light in the process of oxidation of contaminants, such as small aromatic compounds.

3.2. Effect of H_2O_2 concentration on the oxidation

Fig. 3 (a) and (b) show the UV-Vis and the synchronous fluorescence spectra, respectively, recorded during the oxidation of the mixture by UV/H_2O_2, at pH 5.6 and up to 4 h of reaction, with three different initial concentrations of H_2O_2: 0.5 mM, 2.5 mM and 5.0 mM. As shown in Fig. 3, with higher initial H_2O_2 concentrations, higher oxidation rates are obtained. Fig. 3 (a) shows that, at 0 h, higher H_2O_2 concentrations originate higher absorbances, since H_2O_2 contributes to the absorbance of the spectra. After the oxidation starts, higher concentrations of H_2O_2 conduct to lower absorbances. This occurs because, higher H_2O_2 concentrations, originate more hydroxyl radicals, which can react with the compounds and degrade them. However, after 4 h, similar absorbances were obtained for 2.5 mM and 5.0 mM, which suggests that a similar stage of oxidation was obtained with these two concentrations. These conclusions can also be drawn from the analysis of the synchronous fluorescence spectra (Fig. 3 (b)), which suggest that, when using a concentration of H_2O_2 of 0.5 mM, there are still chromophoric compounds in solution after 4 h of reaction, while, for 2.5 mM and 5.0 mM of H_2O_2, no chromophoric compounds remain.

3.3. Effect of pH on the oxidation

To evaluate the influence of the initial pH in the oxidation of the mixture of contaminants by UV/H_2O_2, pH values 4.0, 5.6, and 7.0 were tested. The initial H_2O_2 concentration used was 5.0 mM, and, thus, the maximum reaction time was set for 4 h, which is the time needed to completely degrade the chromophoric compounds with this concentration. The UV-Vis and the synchronous fluorescence spectra obtained during the oxidation of the mixture of contaminants by UV/H_2O_2, for 0 h, 1 h, 2 h, 3 h, and 4 h (see SM, Fig. SM-4 (a) and (b), respectively), show that no relevant differences can be pointed out between the different pH values tested, which suggests that the oxidation of the mixture of contaminants might not be influenced by the initial pH of the solution. Nevertheless, the EEM fluorescence spectra obtained during the oxidation of the mixture for the different pH values (see SM, Figure SM-5) show that, at the initial time (0 h), the fluorescent bands for pH 4.0 display a lower intensity when compared to pH 5.6 and 7.0. This means that the initial fluorescence of the mixture is pH dependent, which is a consequence of the protonation of the compounds. In this case, pH 4.0 has a higher degree of protonation, and presents a lower fluorescence intensity than the other pH values (Sharma and Schulman, 1999). However, during the oxidation reaction, the spectra of the different pH become very similar, which might mean that the pH does not have an influence on the oxidation of the mixture.

To evaluate the differences between pH values, the integrated volume under the surface of the EEM fluorescence spectra was calculated for each reaction time, for the three values of pH, and converted to extent of oxidation, according to Equation 1. The extents of oxidation for each reaction time (0 h, 1 h, 2 h, 3 h and 4 h), and for each pH value (4.0, 5.6 and 7.0) are presented in Fig. 4. As shown in Fig. 4, the extents of oxidation are similar for the three pH's, and apparently different between pH 4.0 and pH 5.6 at the reaction times of 1 h and 2 h. After 1 h, the average extent of oxidation was 50.7% at

pH 5.6, and 30.8% at pH 4.0. Afterwards, at 2 h, the average extent of oxidation was 95.4% at pH 5.6, and 88.1% at pH 4.0. Moreover, the extent of oxidation reached the maximum oxidation rate (at about 100%) for the three pH's within 3 h of reaction. The extents of oxidation obtained were compared using a two-sided Student's *t-test* for a significance level of 5% ($\alpha = 0.05$). The results from the application of the *t-test* to the experimental data are presented in the Table SM-1 of the SM, and it can be concluded that the null hypothesis, which states that there is no difference between the two means, can only be rejected for pH 4.0 vs pH 5.6, for the reaction times of 1 h and 2 h, since t_{stat} > t_{crit} and *p-value* < 0.05. As previously discussed, at a reaction time of 0 h, the EEM fluorescence spectrum of pH 4.0 presents a lower intensity when compared to the other two pH's. Since the extent of oxidation is calculated based on the integrated EEM fluorescence spectra volume, and uses the volume of the spectra of 0 h, the difference between pH 4.0 and 5.6 at the reaction times of 1 h and 2 h can be attributed to the difference in the spectra of 0 h. Nevertheless, when considering a significance level of 0.01, the null hypothesis cannot be rejected for pH 4.0 *vs* pH 5.6 for the reaction time of 1 h. Additionally, for pH 4.0 *vs* pH 5.6, at 2 h, the null hypothesis cannot be rejected at a significance level of 0.01. Considering this information, there is no statistical evidence to affirm that the pH influences the oxidation of the mixture of compounds.

3.4. Optimization of the UV/H_2O_2 process on the oxidation of the mixture of contaminants

The results shown above show the potential of the UV/H_2O_2 process in the degradation of the mixture of contaminants, and that this process is influenced by the reaction time and by the initial H_2O_2 concentration, and, apparently, not influenced by the initial pH of the solutions. Thus, to find the best set of experimental conditions, that return the

best possible outcome (an extent of oxidation near 100 %), to the oxidation of the mixture of contaminants, the optimization of the UV/H_2O_2 process was performed using the Uniform Design. The factors considered for the optimization were those previously studied: reaction time, initial pH and initial H_2O_2 concentration. For that purpose, three factors with three levels were used: 0.5 mM, 2.5 mM and 5.0 mM, for H_2O_2 concentration; 2 h, 4 h and 7 h, for reaction time; and 4.0, 5.6, and 7.0, for pH. The extent of oxidation was used as the response variable. Three replications of the experimental design were made, and the results can be seen in Table 1. As it can be seen in the Table 1, the percentage of oxidation varied from 18% to 100%, and replicas did not present standard deviations higher than 3%. The results were then analyzed using the best subsets regression approach, having been compared all possible models within a second order polynomial framework, which was built on a set of predictors and leaded to the best models for each number of possible predictors. According to Equation 2, the regression analysis considered: three first-order effects, initial H_2O_2 concentration ($[H_2O_2]_0$), time of reaction (t) and initial pH; three interaction effects, specifically, the interaction between H_2O_2 concentration and time of reaction ($[H_2O_2]_0 \times t$), between H_2O_2 concentration and pH ($[H_2O_2]_0 \times pH$), and between time of reaction and pH (t$\times$pH); and three second-order effects, $[H_2O_2]_0^2$, t^2 and pH^2. Through the application of the best subsets regression, eight models were suggested (see SM, Table SM-2). All models contemplated are significant at a 95 % confidence level, but models 7 and 8 display predictor variables ($[H_2O_2]\times pH$, t$\times$pH) with *p-values* higher than 0.05, which means that those predictor variables are not significant in the model in which they are predictors. Values of R^2 close to 1 indicate that most of the variability in the dependent variable is explained by the regression model (Montgomery et al., 2001). However, the R^2 parameter increases by adding terms to the model, regardless of the contribution of

that variable (Montgomery et al., 2001), which makes this parameter not suitable for the choice of the best model. Besides that, R^2 stabilized with more than 5 predictor variables. On the other hand, R^2_{adj} only increases by adding a variable to the model if the addition of the variable reduces the residual mean square (Montgomery et al., 2001), so it is more adequate to use R^2_{adj}, as it only increases if the added predictors improve the model (Manan et al., 2019), and the highest R^2_{adj} belongs to model 5 (0.921). Nevertheless, Olejnik et al. (2000) demonstrated that C_p has more success in identifying the authentic variables than R^2_{adj}, since it is a measure of bias or prediction error. Therefore, small values of C_p are desirable (Montgomery et al., 2001), and the smallest value of Mallow's C_p belongs to model 5, which means that this model is more precise than the others. Given that the smallest C_p and the highest R^2_{adj} values belong to model 5, this model was chosen as the "best", from the models resultant from the application of best subsets regression. This model considers the initial H_2O_2 concentration, reaction time, the interaction between these two and their quadratic forms as variables. This means that the initial pH of the solution is not significant for the oxidation of the mixture, which is in agreement with the previous section, where it was stated that there was no statistical evidence to conclude that the pH had influence on the oxidation of the mixture of contaminants.

A summary of the chosen model is displayed in Table 2, where information about the sum of squares, mean square, degrees of freedom, F and p-values, R^2 and R^2_{adj} are presented. As shown in the table, the model presents a good fit to the experimental data, since the R^2_{adj} is 0.921, which means that 92.1% of the results can be explained by the model. Moreover, the model has a high significance, since F_{crit} (2.53) < $F_{(5,30)}$ (82.9), and its p-value is inferior to 0.05 (p-value < 0.001). The sum of squares (SS) of the model and of each variable allowed the evaluation of their significance (p-value < 0.05).

Therefore, the relationship between the extent of oxidation of the mixture and the independent variables is given by:

$Extent\ of\ oxidation\ (\%)$

$$= -31.20 + 35.01 \times [H_2O_2] + 26.82 \times t - 2.526 \times [H_2O_2]^2 - 1.402$$
$$\times t^2 - 3.084 \times [H_2O_2] \times t \qquad (4)$$

where $[H_2O_2]$ is the initial concentration of H_2O_2 (mM) and t is the reaction time (h). The coefficients in this equation reveal that the concentration of H_2O_2 and that the time of reaction have a positive influence on the extent of oxidation: an increase in the H_2O_2 concentration, or in the reaction time leads to higher percentages of extent of oxidation. The relationship between the predicted and experimental values of the extent of oxidation is linear ($R^2 = 0.9377$; see SM, Fig. SM 5), indicating that there is a strong correlation between the model's predictions and its actual results, and that the proposed model is adequate. This relationship can be clearly seen in Fig. 5 (a) and (b), which shows the response surface model obtained and the experimental data, both plotted with the Working-Hotelling surface confidence intervals, at a 95% confidence level. As shown in Fig. 5, at a reaction time of 2 h and at an H_2O_2 concentration of 0.5 mM, the response surface model presents a low percentage of extent of oxidation (about 20%), that increases as the H_2O_2 concentration increases, or as the reaction time increases. Furthermore, it is worth to mention that the mean values of the experimental data are within the surface confidence intervals. On the other hand, the individual values are within the confidence intervals, except for a concentration of H_2O_2 of 0.5 mM, a pH of 5.6 and a reaction time of 2 h, and for H_2O_2 of 2.5 mM, a pH of 4.0 and a reaction time of 2 h. However, the values that are out of the confidence intervals are not statistically different from the values that are contained within the intervals (Dixon's test; $\alpha = 0.05$),

corroborating that the experimental data are well described by the response surface model.

The extent of oxidation was optimized based on the equation obtained for the model, and an equilibrium between H_2O_2 concentration and reaction time was desired. The minimum H_2O_2 concentration for the maximum reaction time of 4 h, which translated into extents of oxidation equal or higher than 99.5%, was searched, resulting the optimum conditions for the oxidation of the mixture of contaminants in an H_2O_2 concentration of 3.1 mM and a reaction time of 4 h.

3.5. Oxidation of the mixture of contaminants by the UV/H_2O_2 process in rainwater samples

The effect of the oxidation of the mixture of contaminants by the UV/H_2O_2 process in rainwater samples, was assessed in experiments with two rainwater samples spiked with the mixture of contaminants at their natural pH, namely pH 5.2 and pH 5.4, for samples 1 and 2, respectively. These experiments were performed with a concentration of H_2O_2 of 5.0 mM, to allow the comparison with the previous results with the model solutions, for the following reaction times: 0 h, 2 h, and 4 h. A final reaction time of 4 h was chosen so that everything would surely be oxidized by the end of this time, similar to what was observed for model solutions. As control, the following experiments were performed: samples spiked with the mixture of contaminants, and without H_2O_2; samples with H_2O_2 at a concentration of 5.0 mM; and samples without H_2O_2. The UV-Vis spectra resultant from these experiments are presented in the SM, Fig. SM-7. The UV-Vis spectra of the two samples (at 0 h for a concentration of H_2O_2 of 0 mM) are similar to those obtained by Santos et al. (2019) for rainwater samples, decreasing the absorbance of both samples as the wavelength increases. There are no changes with the

time in the spectra that correspond to the experiments with samples not spiked with the mixture of contaminants and without H_2O_2, which reveals that there was no oxidation in this case. In the spectra obtained in the experiments with the addition of H_2O_2 to the samples, but without these being spiked with the mixture, the absorbance significantly increased when compared to the spectra without H_2O_2, but they did not change with the course of the reaction. Concerning the spectra resultant from the addition of the mixture of contaminants to the samples, but without H_2O_2, they reveal an absorption band at 252 nm at 0 h, which moves to a longer wavelength, 290 nm, after 2 h of reaction. After 4 h of reaction, its absorbance slightly diminishes. These alterations suggest that the compounds are being transformed, similar to what happened in the oxidation with model solutions, where the main absorbance band moved to longer wavelengths. Regarding the spectra obtained for the samples spiked with the mixture of contaminants when H_2O_2 was added in a concentration of 5 mM with the course of the reaction, the compounds are degraded, as the absorbance of the spectra decreases with time. At a reaction time of 4 h, sample 1 seems to have been more oxidized than sample 2.

Fig. 6 (a) and (b) display the EEM fluorescence spectra obtained during the oxidation of samples 1 and 2, and of samples 1 and 2 spiked with the mixture of contaminants, by UV/H_2O_2, and up to 4 h of reaction, as well as for the controls without H_2O_2. The EEM spectrum of samples 1 and 2 shows four fluorescent bands with a low fluorescent intensity, located as similar locations. One is located near 240 nm of excitation and 410 nm of emission wavelength, generally attributed to humic-like compounds (A); other is located near 290 nm of excitation and 420 nm of emission wavelength, generally assigned to marine humic-like compounds (M); and two bands located near 230 nm of excitation and 335 nm of emission wavelength and near 280 nm of excitation and 335 nm of emission wavelength, usually assigned to protein-like compounds, such as

tryptophan (T_1 and T_2, respectively) (Santos et al., 2013). The more intense band in Sample 1 is band A, and T_1 in Sample 2. Nevertheless, band A is more intense than band M in both samples.

The EEM spectra resultant from the oxidation of the samples not spiked with the mixture and without H_2O_2 suggest that there was some oxidation of the compounds in solution, since their intensity decreased throughout time. When adding H_2O_2, after 2 h of reaction time, all chromophoric compounds were degraded, for both samples. In the case where the samples were spiked with a mixture of contaminants, but without H_2O_2 in solution, the fluorescence spectra of 0 h, suggest the presence of two fluorescent bands, one located at 270 nm of excitation and 335 nm of emission wavelength, and the other submerged in this one, which were also identified in the experiments with the model solutions. After 2 h, two new fluorescent bands appear, one located at 240 nm of excitation and 420 nm of emission, and other at 300 nm of excitation and 415 nm of emission wavelength, which also appear in the spectra of the oxidation of the model solutions, suggesting that the same compounds are being formed. After 4 h, the intensity of these bands increases, like in the case of the model solutions, meaning that there are more chromophoric compounds that fluoresce in that region being formed. These observations suggest that UV light, on its own, is able to oxidize the samples spiked with the mixture, at some extent. At last, the oxidation of the samples spiked with the mixture, by the UV/H_2O_2 process, conducted to the complete oxidation of the samples in 4 h, similar to what was observed for the model solutions. However, after 2 h of reaction, sample 2 seems to have been more degraded than sample 1, suggesting that the matrix could be influencing the oxidation. When comparing the spectra from the oxidation of the sample spiked with the mixture only by UV light, to those of the oxidation of the sample spiked with the mixture by the UV/H_2O_2 process, it is clear that

UV light causes some oxidation, but that the addition of H_2O_2 significantly increases the rate of oxidation, due to the formation of hydroxyl radicals, that attack and degrade the compounds in solution. Santos et al. (2019) also observed that H_2O_2 increases the extent of oxidation of benzoic acid in rainwater in the presence of sunlight, when compared to the same oxidation without H_2O_2. These findings corroborate that the photogeneration of hydroxyl radical from H_2O_2 is an important factor for the degradation of contaminants in rainwater.

The optimal conditions (3.1 mM for H_2O_2 concentration and 4 h for reaction time), found in the previous section in the optimization of the UV/H_2O_2 process for the oxidation of a mixture of contaminants, were also applied to the samples spiked with the mixture of contaminants. The experiments were performed in duplicates, at their natural pH values. The results were an average extent of oxidation of 99.8% for sample 1, and of 99.5% for sample 2. These results are in accordance with what was predicted by the equation of the model, obtained in the previous section, which estimates that, with the optimum conditions, an extent of oxidation higher than 99.5% is obtained. These findings suggest that the model obtained, for the aforementioned conditions (3.1 mM for H_2O_2 concentration and 4 h for reaction time), can be used for the oxidation of contaminants in real samples.

3.5. Implications of the study

Some chemicals arising in rainwater are of health concern. Rainwater quality according to the World Health Organization (WHO) drinking water guideline requires its treatment before use. To remove organic contaminants from rainwater, such as small aromatic compounds, a treatment process is required. The proposed UV/H_2O_2 process can be applied after collection of rainwater, either by roofing catchment or in tanks for

such purpose. Since the pH value of rainwater does not affect the rainwater treatment by the UV/H_2O_2 process, which constitutes an advantage, the pH adjustment is not required and the process can be applied in a simple away. Moreover, other important advantages of the UV/H_2O_2 process are that it does not cause secondary water pollution at the end of reaction (the organic substances are oxidized to carbon dioxide and water) and that it is a process with easy operationalization and few safety precautions. Although the scale up of the process was not evaluated, considering that, after filtration, rainwater can be in a tank where the treatment process is performed, according to the rainwater amount, the necessary amount of H_2O_2 is added and the rainwater is subjected to an adequate time of UV radiation, which should be foreseen by the model. Therefore, enhancing the efficiency of the UV/H_2O_2 process is desired, through the application of the optimum H_2O_2 dose and reaction time to remove approximately 100 % of the small aromatic compounds present in the rainwater, in order to reduce chemical and energy costs for the removal. Chemical and energy costs, H_2O_2 30 % (w/w) and UV lamp (6 W), respectively, can be estimated in accordance with their unit costs (0.146 €/mL for H_2O_2 30 % (w/w) from Sigma-Aldrich (https://www.sigmaaldrich.com/PT/en/product/sigald/216763; accessed 28 December 2121) and 0.14 €/kWh for electricity in Portugal). Accordingly with the model found, the operating costs of the treatment process include the addition of 0.5–5.0 mM H_2O_2 and UV radiation for 2-7 h. Assuming the treatment of a 1 L rainwater sample, the cost would be 0.013 € when 0.5 mM H_2O_2 is used for a 7 h water treatment (less H_2O_2 is added taking the most time to achieve a full degradation of the small aromatic compounds), and 0.076 € when 5.0 mM H_2O_2 is used in the fastest process (2 h), which suggests that the UV/H_2O_2 process may be economically feasible on the treatment of a higher rainwater amount. Nevertheless, a study of the scale up of the process (with an

automatic technology) and respective cost analysis should be performed in the future, also including the investment cost for apparatus and buildings.

4. Conclusions

The study and optimization of the oxidation of a mixture of small aromatic compounds in rainwater by the UV/H_2O_2 process led to the following main conclusions:

- The UV-Vis and fluorescence spectra obtained during the oxidation process suggest the formation of new chromophoric compounds, which are then degraded. The rate of oxidation is not affected by the pH of the solution, but it is affected by the initial H_2O_2 concentration, since higher H_2O_2 concentrations lead to higher oxidation rates.

- The model achieved by response surface methodology is a second-order polynomial surface, where initial H_2O_2 concentration, reaction time, the interaction of these two factors and their quadratic forms are the variables. The model was able to predict the extents of contaminants' oxidation in rainwater efficiently, despite results showing that the rainwater matrix could be affecting the oxidation.

- This research showed, for the first time, the application of a response surface model to the optimization of the rainwater treatment with the UV/H_2O_2 process, for the removal of organic contaminants. Such finding could help to improve the water resources sustainable management, specifically by the use of treated rainwater by this process in buildings for domestic purposes.

Credit Author Statement

Mónica P.S. Ferreira: Methodology, Validation, Formal analysis, Investigation, Writing - Original Draft, Writing - Review & Editing, Visualization. Patrícia S.M. Santos: Conceptualization, Methodology, Validation, Investigation, Writing - Original Draft, Writing - Review & Editing, Visualization, Supervision, Project administration, Funding acquisition. Armando C. Duarte: Methodology, Validation, Resources, Writing - Review & Editing, Supervision, Funding acquisition.

Declaration of interests
The authors declare that they have no known competing financial interests or personal relationships that could have appeared to influence the work reported in this paper.
The authors declare the following financial interests/personal relationships which may be considered as potential competing interests

Supplementary data

Supplementary material

References

Boris, A. J., Desyaterik, Y., Collett, J. L., 2015. Reprint of "How do components of real cloud water affect aqueous pyruvate oxidation?". Atmos. Res. 151, 52–63. https://doi.org/10.1016/j.atmosres.2014.02.004.

Council Directive 98/83/EC of 3 November 1998 on the quality of water intended for human consumption. Off. J. 330, 0032-0054.

Deming, S. N., Morgan, S. L., 1987. Experimental design: a chemometric approach, first ed., Elsevier, Amsterdam.

Deng, Y., Zhang, K., Chen, H., Wu, T., Krzyaniak, M., Wellons, A., Bolla, D., Douglas, K., Zuo, Y., 2006. Iron-catalyzed photochemical transformation of benzoic acid in atmospheric liquids: Product identification and reaction mechanisms. Atmos. Environ. 40, 3665–3676. https://doi.org/10.1016/j.atmosenv.2006.03.019.

Ding, X., Gutierrez, L., Croue, J.-P., Li, M., Wang, L., Wang, Y., 2020. Hydroxyl and sulfate radical-based oxidation of RhB dye in UV/H_2O_2 and UV/persulfate systems: Kinetics, mechanisms, and comparison. Chemosphere 253, 126655. https://doi.org/10.1016/j.chemosphere.2020.126655.

European Environment Agency, 2009. Water Resources across Europe – Confronting Water Scarcity and Drought. Copenhagen.

Environment Agengy, 2010. Harvesting rainwater for domestic uses: an information guide. Bristol.

Fiorentino, A., Lofrano, G., Cucciniello, R., Carotenuto, M., Motta, O., Proto, A., Rizzo, L., 2021. Disinfection of roof harvested rainwater inoculated with E. coli and Enteococcus and post-tretment bacterial regrowth: Conventional vs solar driven advanced oxidation processes. Sci. Total Environ. 801, 149763. https://doi.org/10.1016/j.scitotenv.2021.149763.

Graham, B., Mayol-Bracero, O. L., Guyon, P., Roberts, G. C., Decesari, S., Facchini, M. C., Artaxo, P., Maenhaut, W., Koll, P., Andreae, M. O., 2002. Water-soluble organic compounds in biomass burning aerosols over Amazonia 1. Characterization by NMR and GC-MS. J.Geophys. Res., 107(D20), 8047. https://doi.org/10.1029/2001JD000336.

Kasiri, M. B., Aleboyeh, H., Aleboyeh, A., 2008. Modeling and Optimization of Heterogeneous Photo-Fenton Process with Response Surface Methodology and Artificial Neural Networks. Environ. Sci. Technol., 42(21), 7970–7975.

https://doi.org/10.1021/es801372q.

Kokkinos, P., Venieri, D., Mantzavinos, D., 2021. Advanced Oxidation Processes for Water and Wastewater Viral Disinfection. A Systematic Review. Food Environ. Virol. 13, 283-302. https://doi.org/10.1007/s12560-021-09481-1.

Li, R., Lin, D. K. J., Chen, Y., 2004. Uniform design: design, analysis and applications. Int. J. Mater. Prod. Tec. 20 (1-3), 101-114. https://doi.org/10.1504/IJMPT.2004.003915.

Li, Z., Chen, W., Li, J., Yue, S., 2016. Advanced treatment of rainwater by H_2O_2/UV process. Progress in Civil, Architectural and Hydraulic Engineering - Selected Papers of the 4th International Conference on Civil, Architectural and Hydraulic Engineering, ICCAHE 2015, 1371-1376.

Liu, Z., Lin, Y.-L., Chu, W.-H., Xu, B., Zhang, T.-Y., Hu, C.-Y., Cao, T.-C., Gao, N.-Y., Dong, C.-D., 2020. Comparison of different disinfection processes for controlling disinfection by-product formation in rainwater. J. Hazard Mater. 385, 121618. https://doi.org/10.1016/j.jhazmat.2019.121618.

Manan, T. S. B. A., Khan, T., Sivapalan, S., Jusoh, H., Sapari, N., Sarwono, A., Ramli, R. M., Harimurti, S., Beddu, S., Sadon, S. N., Kamal, N. L. M., Malakahmad, A., 2019. Application of response surface methodology for the optimization of polycyclic aromatic hydrocarbons degradation from potable water using photo-Fenton oxidation process. Sci. Total Environ. 665, 196–212. https://doi.org/10.1016/j.scitotenv.2019.02.060.

Mangalgiri, K., Cheng, Z., Cervantes, S., Spencer, S., Liu, H., 2021. UV-based advanced oxidation of dissolved organic matter in reverse osmosis concentrate from a potable water reuse facility: A Parallel-Factor (PARAFAC) analysis approach. Water Res. 204, 117585. https://doi.org/10.1016/j.watres.2021.117585.

Montgomery, D. C., Peck, E. A., Vining, G. G., 2001. Introduction to linear regression analysis, third ed, John Wiley & Sons, Inc, New York.

Mao., J., Xia, B., Zhou, Y., Zhang, X., Zhang, W., Xia, S., 2021. Effect of roof materials and weather patterns on the quality of harvested rainwater in Shanghai, China. J. Clean. Prod. 279, 123419. https://doi.org/10.1016/j.jclepro.2020.123419.

Olejnik, S., Mills, J., Keselman, H., 2000. Using Wherry's Adjusted R and Mallow's Cp for Model Selection From All Possible Regressions. J. Exp. Educ. 68(4), 365–380. https://doi.org/10.1080/00220970009600643.

Polyokova, O.V., Artaev, V.B, Lebedev, A.T., 2018. Priority and emerging ollutants in the Moscow rain. Sci. Total Environ. 645, 1126-1134. https://doi.org/10.1016/j.scitotenv.2018.07.215.

Santos, P.S.M., Otero, M., Santos, E.B.H., Duarte, A.C., 2011. Chemical composition of rainwater at a coastal town on the southwest of Europe: what changes in 20 years? Sci. Total Environ. 409, 3548-3553. https://doi.org/10.1016/j.scitotenv.2011.05.031.

Santos, P.S.M., Santos, B.H.E., Duarte, A.C., 2013. Seasonal and air mass trajectory effects on dissolved organic matter of bulk deposition at a coastal town in south-western Europe. Environ. Sci. Pollut. Res. 20, 227-237. https://doi.org/10.1007%2Fs11356-012-0971-4.

Santos, P.S.M., Duarte, A.C., 2015. Fenton-like oxidation of small aromatic acids from biomass burning in water and in the absence of light: implications for atmospheric chemistry. Chemosphere 119, 786-793. https://doi.org/10.1016/j.chemosphere.2014.08.024.

Santos, G.T.A.D., Santos, P.S.M., Duarte, A.C., 2016. Vanillic and syringic acids from biomass burning: Behaviour duting Fenton-like oxidation in atmospheric aqueous

phase and in the absence of light. J. Hazard Mater. 313, 201–208.

https://doi.org/10.1016/j.jhazmat.2016.04.006.

Santos, P.S.M., Cardoso, H.B., Rocha-Santos, T.A.P., Duarte, A. C., 2019. Oxidation of

benzoic acid from biomass burning in atmospheric waters. Environ. Pollution 244,

693–704. https://doi.org/10.1016/j.envpol.2018.10.059.

Santos, P.S.M., Santos, G.T.A.D., Cachada, A., Patinha, C., Coimbra, M.A., Coelho, E.,

Duarte, A. C., 2021. Sources of carbohydrates on bulk deposition in South-

Western of Europe. Chemosphere 263, 127982.

https://doi.org/10.1016/j.chemosphere.2020.127982.

Seinfeld, J. H., Pandis, S. N., 2006. Atmospheric Chemistry and Physics: From Air

Pollution to Climate Change, 2nd ed., John Wiley & Sons, Inc., New Jersey.

Simoneit, B. R. T., 2002. Biomass burning a review of organic tracers for smoke from

incomplete combustion. Appl. Geochem. 17, 129-162.

https://doi.org/10.1016/S0883-2927(01)00061-0.

Sharma, A., Schulman, S. G., 1999. Introduction to fluorescence spectroscopy. John

Wiley & Sons, Inc, New York.

Vione, D., Maurino, V., Minero, C., Duncianu, M., Olariu, R. I., Arsene, C., Sarakha,

M., Mailhot, G., 2009. Assessing the transformation kinetics of 2- and 4-

nitrophenol in the atmospheric aqueous phase. Implications for the distribution of

both nitroisomers in the atmosphere. Atmos. Environ. 43(14), 2321–2327.

https://doi.org/10.1016/j.atmosenv.2009.01.025.

Vione, D., Maurino, V., Minero, C., Pelizzetti, E., Harrison, M. A. J., Olariu, R.-I.,

Arsene, C., 2006. Photochemical reactions in the tropospheric aqueous phase and

on particulate matter. Chem. Soc. Rev. , 35, 441-453.

https://doi.org/10.1039/B510796M.

Wang, C., Moore, N., Bircher, K., Andrews, S., Hofmann, R., 2019. Full-scale

comparison of UV/H_2O_2 and UV/Cl_2 advanced oxidation: The degradation of

micropollutant surrogates and the formation of disinfection byproducts. Water Res.

161, 448-458. https://doi.org/10.1016/j.watres.2019.06.033.

Williams, D. H., Fleming, I., 1989. Spectroscopic methods in organic chemistry, 4th

ed., McGraw-Hill, London.

Zhao, J., Wang, Y., Liu, H., Wu, Y., Dong, W., 2022. Discrepant oxidation behavior of

ferric ion and hydroxyl radical on syringic acid and vanillic acid in atmospheric

Fenton-like system. Chemosphere 287, 132022.

https://doi.org/10.1016/j.chemosphere.2021.132022.

Zuo, Y., Holgné, J., 1992. Formation of Hydrogen Peroxide and Depletion of Oxalic

Acid in Atmospheric Water by Photolysis of Iron(III)-Oxalato Complexes. Environ.

Sci. Technol. 26(5), 1014–1022. http://doi.org/10.1021/es00029a022.

Table 1. Results from the experimental design, expressed as extent of oxidation (%) for the three replicates, and respective level for each factor ([H_2O_2], t, pH).

	Factors			Extent of oxidation (%)		
Run order	[H_2O_2] (mM)	t (h)	pH	First replica	Second replica	Third replica
1	0.5	4	7.0	65.6	72.3	69.1
2	2.5	7	4.0	99.9	100.0	100.0
3	5.0	7	5.6	100.0	100.0	100.0
4	5.0	2	5.6	99.1	95.8	97.9
5	2.5	2	7.0	74.3	81.2	75.6
6	5.0	4	4.0	99.9	100.0	100.0
7	0.5	2	5.6	21.8	19.1	18.0
8	2.5	2	4.0	79.9	82.7	79.2

9	2.5	7	7.0	100.0	100.0	100.0
10	5.0	4	7.0	100.0	100.0	100.0
11	0.5	7	5.6	93.6	99.5	98.2
12	0.5	4	4.0	66.4	70.8	65.6

Table 2. Model summary, where *SS* stands for sum of squares, *DF* for degree of freedom, and *MS* for mean square. *F* and *p-values*, R^2, R^2_{adj} and the coefficients of each variable in the model are also present.

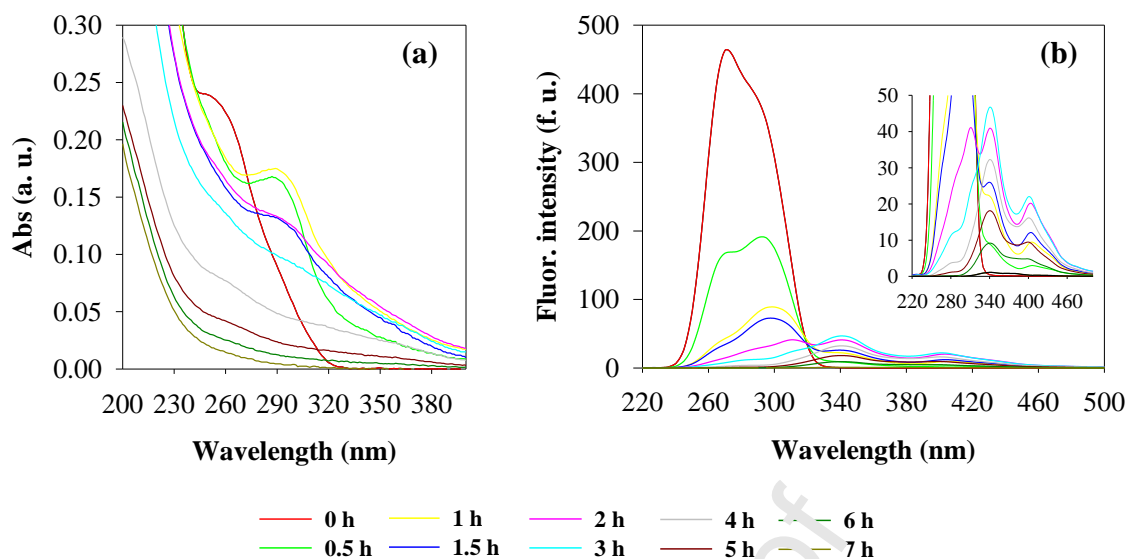|	*SS*	*DF*	*MS*	**Coefficient**	*F*	*p-value*	R^2	R^2_{adj}
Corrected model	17801	5	3560		82.9	<0.001	0.933	0.921
Intercept	425	1	425		9.90	0.004		
Constant				-31.20				
$[H_2O_2]$	4717	11	4717	35.01	110	<0.001		
t	1747	1	1747	26.82	40.7	<0.001		
$[H_2O_2]^2$	954	1	954	-2.526	22.2	<0.001		
t^2	420	1	420	-1.402	9.79	0.004		
$[H_2O_2] \times t$	3706	1	3706	-3.084	86.3	<0.001		
Error	1288	20	42.9					
Total	273201	36						
Corrected Total	19089	35						

Figure 1. Absorbance spectra (average spectra) **(a)** and synchronous fluorescence spectra ($\Delta\lambda = 60$ nm) **(b)** of the mixture of the three acids during the oxidation by UV/H_2O_2, with $[H_2O_2]_0$ of 0.5 mM and at pH 5.6.
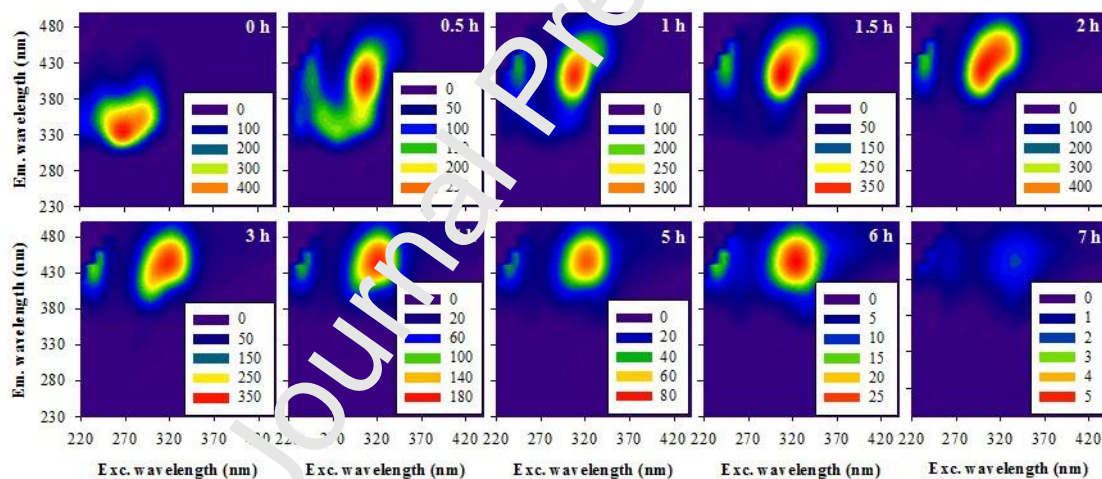

Figure 2. Excitation-emission matrix (EEM) fluorescence spectra of the mixture of the three contaminants during the oxidation by UV/H_2O_2, at pH 5.6, with $[H_2O_2]_0$ of 0.5 mM, and for the oxidation times of: 0 h, 0.5 h, 1 h, 1.5 h, 2 h, 3 h, 4 h, 5 h, 6 h and 7 h.
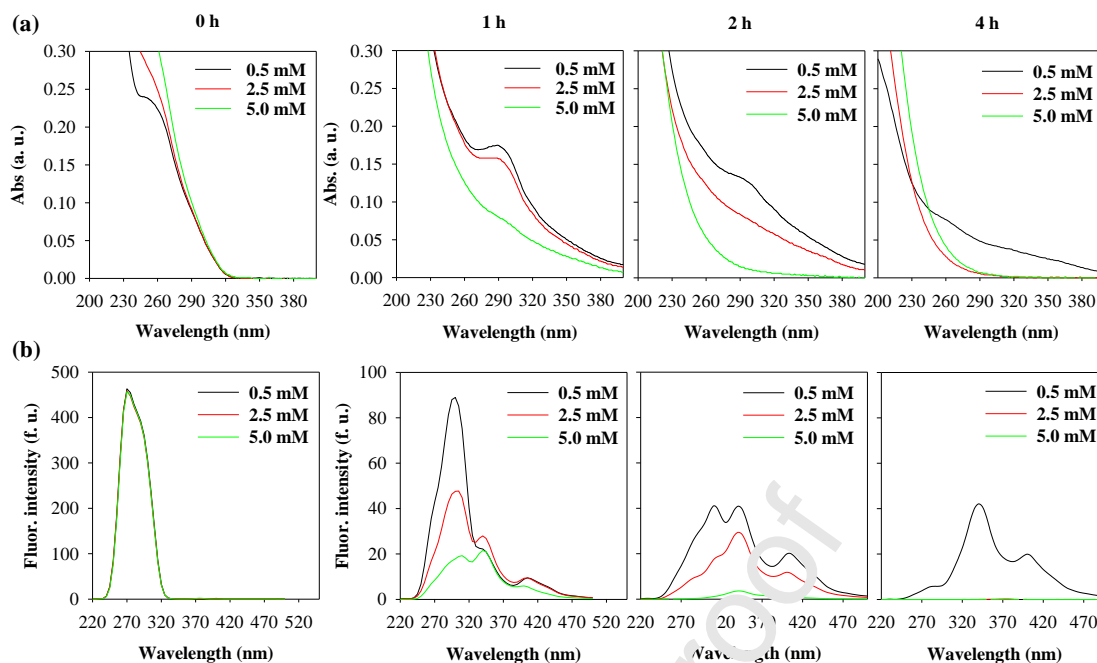
Figure 3. UV-Vis spectra **(a)** and synchronous fluorescence spectra ($\Delta\lambda = 60$ nm) **(b)** during the oxidation of the mixture of contaminants by UV/H_2O_2, at pH 5.6, for reaction times of 0 h, 1 h, 2 h and 4 h, and with [H_2O_2] of 0.5 mM, 2.5 mM and 5.0 mM.
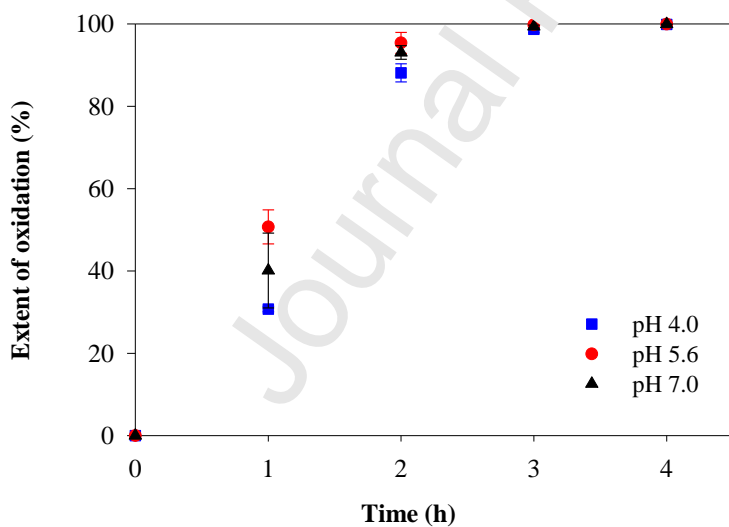

Figure 4. Extent of oxidation (%; average values) of the mixture of compounds during oxidation by UV/H_2O_2, with [H_2O_2]$_0$ of 5 mM, at pH 4.0, 5.6 and 7.0, and for the following reaction times: 0 h, 1 h, 2 h, 3 h and 4 h.
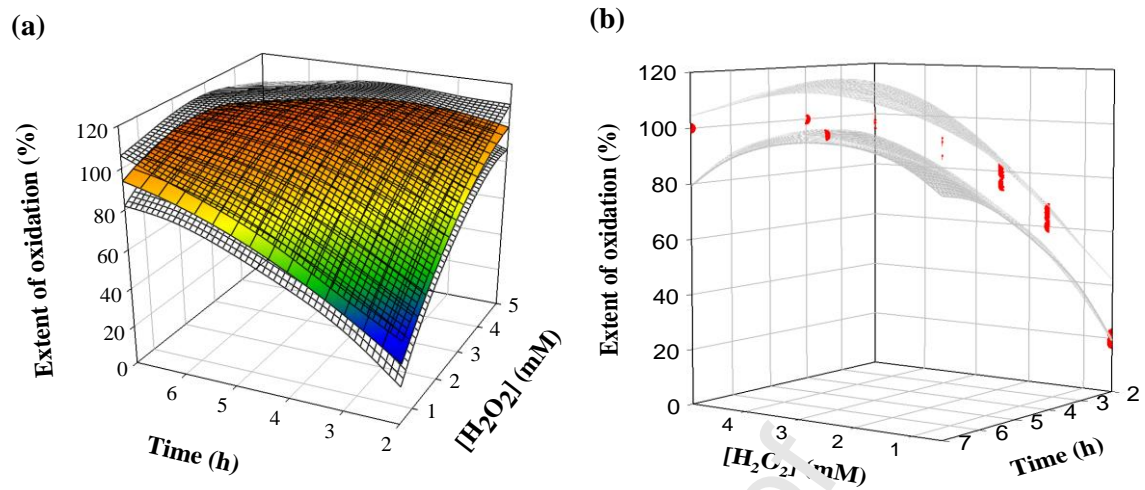
(a)

(b)

Figure 5. (a) Response surface model with the associated Working-Hotelling surface confidence intervals at a 95 % confidence level. **(b)** Experimental data with the Working-Hotelling surface confidence intervals at a 95 % confidence level.
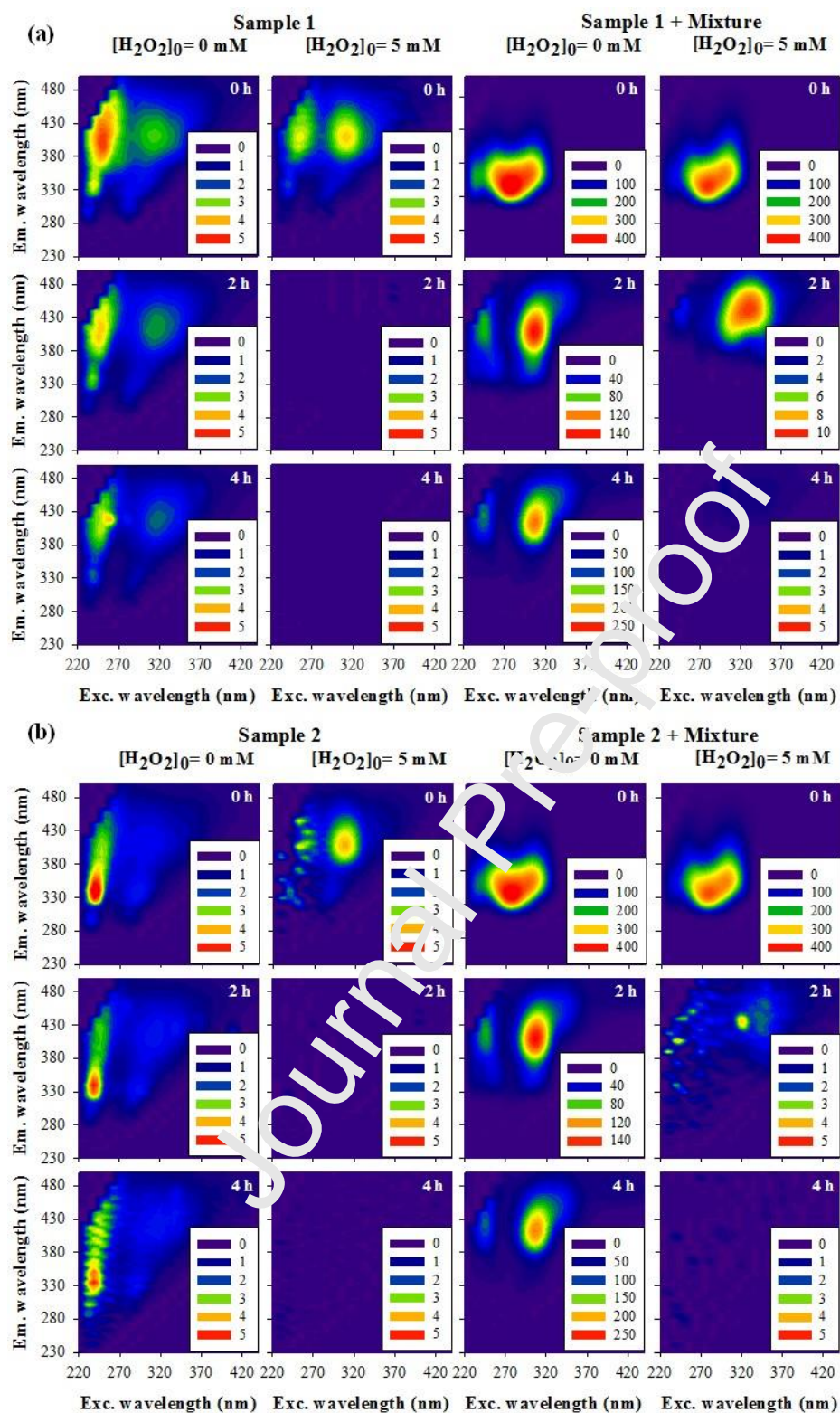
Figure 6. Excitation-Emission matrix (EEM) fluorescence spectra during the oxidation of rainwater samples 1 **(a)** and 2 **(b)** at their natural pH (5.2 and 5.4, respectively) and for 0 h, 2 h and 4 h: not spiked with the mixture of contaminants and H_2O_2 ($[H_2O_2]_0 = 0$ mM; by UV); not spiked with the mixture of contaminants, but spiked with H_2O_2 ($[H_2O_2]_0 = 5$ mM; by UV/H_2O_2); spiked with the mixture of contaminants, and not spiked with H_2O_2 ($[H_2O_2]_0 = 0$ mM; by UV); and spiked with the mixture of contaminants and H_2O_2 ($[H_2O_2]_0 = 5$ mM; by UV/H_2O_2).

Graphical Abstract
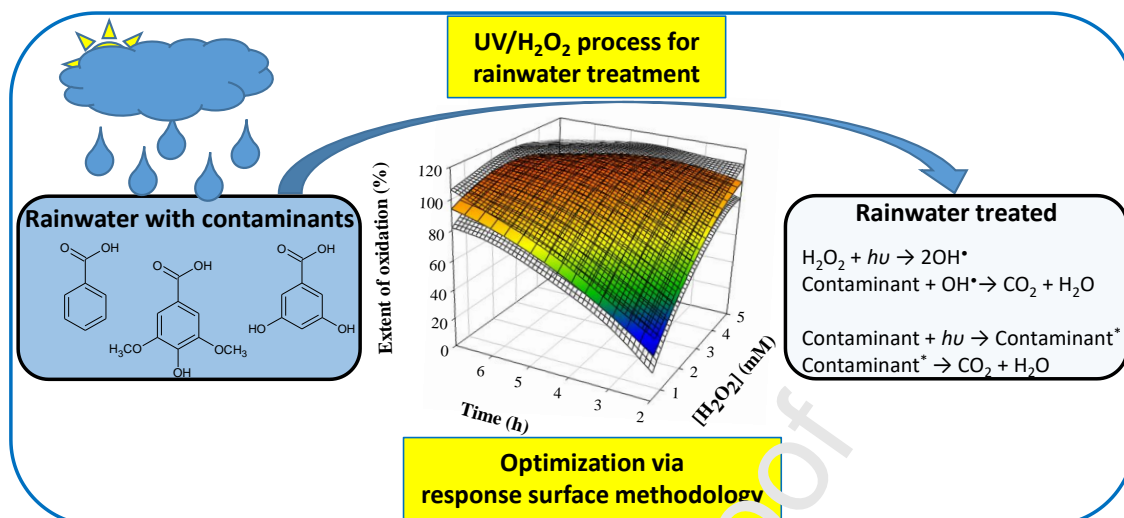
Highlights

- The UV/H$_2$O$_2$ process degrades small aromatic compounds in rainwater efficiently.
- The rate of oxidation of contaminants is not affected by the pH of the solution.
- The rainwater matrix may affect the oxidation of the mixture of contaminants.
- The response surface model predicts the oxidation extent of contaminants in rainwater.
- The UV/H$_2$O$_2$ process may be considered an alternative for rainwater treatment.